Synthesis and characterization of local impurities doped lead chloride (PbCl₂) crystal in silica gel

Don Okpala.V. Uche.

Department of Industrial Physics, Anambra State University, Uli, Anambra State, Nigeria
_____

ABSTRACT

The optical properties of local impurities doped lead chloride ($PbCl_2$) have been studied by sol gel technique. The optical properties of the materials were determined using a JENWAY 6405 UV-VIS spectrophotometer operating at a wavelength range of 200nm to 1200nm at an interval of 5nm. It was observed that the crystals are optically transparent. The average refractive index (n) is between 0.6 and 2.9. The band gaps are from 3.2 to 4.3 showing that they are wide band gap materials and are good refractory materials for electronics and solar energy applications.

Key words: Sol gel, Optical properties, Silica model and Local impurities.
_____

INTRODUCTION

Lead chloride ($PbCl_2$) is a halide crystal which occurs naturally in the form of mineral cotunnite. It is used in the production of infra red transmitting glass and basic chloride of lead known as patteson's white lead [1], ornamental glass called aurene glass, stained glass. It is also used as an intermediate in refining bismuth (Bi) ore, it is used in the synthesis of organometallic (metallecene or plumbocenes), lead titanate and barium titanate [2, 3]. The structure of $PbCl_2$ is orthorhombic dipyramidal. In this study, sol-gel method was used. Sol gel is a wet chemical technique widely used in the fields of materials science and ceramic engineering primarily for the fabrication of materials starting from a chemical solution which acts as the precursor for an integrate network (or gel) of either discrete particle or network of polymers, Allman III [4].

Dopants from local materials (Bamboo, Raffia, Potash).
The advancement in nanotechnology has called for the manipulation of the chemistry of materials. Nano technology is the engineering and fabrication of materials with structures smaller than 100nm or one tenth of a micron. A nano metre is one over one million or one thousandth of a micron. It is about the size of six carbon atoms aligned or 10 hydrogen atoms. It is also about 60,000 times smaller than the diameter of a human hair. In nano technology manufacturing we use either top–down or bottom-up [5]. Top-down manufacturing starts with bulk materials which are whittled down, until the features are left in nano scale. Bottom up involves creating materials from individual atoms or molecules and then joining them together in a specific fashion. In this research work local dopants were produced using top-down approach.

Wood is largely made up of cellulose, which is in turn composed of repeating units of glucose, a simple sugar. Cellulose is composed of carbon, hydrogen and oxygen. When wood is burnt, the cellulose is oxidized to carbon dioxide and water. The remaining ashes contain a lot of elemental carbon in the form of soot. Soot is a colloidal carbon. It is in nano dimensions and has been used for centuries as pigments in inks, paints and as a reinforcing agent in rubber (tires) [5]. It is an approximate perfect black body and as such can be widely employed in solar energy technology. This has prompted us in this research work to consider locally produced dopant of about nanostructure to see how they permeate into the fabrics of said crystals.

(a) Bamboo

Bamboo is the most marvelous plant in nature. Bamboo is stronger than wood or timber in tension and compression. Chemical analysis reveals that bamboo has about 1.3% ash, 4.6% ethanol-toluene, 26.1% lignin, 49.7% cellulose, 27.7% [6]. In Hiroshima, Japan the only plant which survived the radiation of the atomic bomb in 1945 was a bamboo plant. In Costa Rica, a building made with bamboo withstood earthquake. It is used in many applications viz; in building it can be used as roof, floor, walls, scaffolds and supports in road construction as bridges. In power generation it is used as check dams in rivers. It is also used in agriculture as check dams in rivers, organic fertilizer, and preservative medium. Its charcoal absorbs radiation like nuclear reactor etc.

(b) Raffia

The epidemis of the leaflet is the fiber and has been used to fabricate many ethnographical items, [7]. Scanning electron microscopy revealed a layered structure: a top layer with a tile-like structure and a bottom layer with a honey comb-like structure. X-ray diffraction shows the presence of cellulose I_B with crystallinity index of 64%. The fiber density is 0.75+0.07, conferring to it the highest known specific mechanical properties among all vegetable fibers, [8].

(c) Potash

Potash is a term coined by early American settlers who produced potassium carbonate by evaporating water filtered through wood ashes. The ash like crystalline residue remaining in the large iron pots was called 'potash' and was used in making soap. Potash (or carbonate of potash) is an impure form of potassium carbonate (K_2CO_3) mixed with other potassium salt. Potash has been used since antiquity in the manufacture of soap, glass and fertilizer, [9]. Local potash is got by burning woods like tree fiber (ngu).

MATERIALS AND METHODS

In growing ($PbCl_2$), 100ml beaker was added with 25ml of sodium silicate solution of pH greater than eleven. It was titrated with some quantity of 1M of tartaric acid. The mixture forms gel at about pH 8. The set gel was added with 20ml of 1M of lead nitrate solution to give lead tartan ate as in equation (1.1),

$$Pb(NO_3)_2 + H_6C_4O_6 \rightarrow PbH_4O_6 + 2HNO_3 \ldots\ldots\ldots\ldots\ldots.(1.1)$$
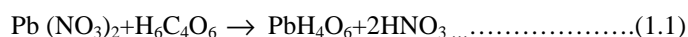
The lead tartanate is generated in the gel as a white column, ring system of gradually increasing thickness. The precipitation of lead tartanate completed within a fortnight. 20ml of 1N of hydrochloric acid (HCl) and a pipette drop of locally produced impurities were placed over the set gel to give,

$$PbH_4C_4O_6 + 2HCl \rightarrow PbCl_2 + H_6C_4O_6 \ldots\ldots\ldots\ldots\ldots\ldots (1.2), [10].$$

The HCl reacted with the colloidal precipitate of lead tartanate producing lead chloride ($PbCl_2$) which grew down into the gel as luminescent needles, [10]. The grown crystals were dried and adequately described through optical characterization (UV-VIS analysis) and structural analysis (XRD). The table of values for the precursors is shown in figure 1.

Table 1: The Precursors

Samp.	Amount of (Na_2SiO_3) (g)	Amount of $Pb(NO_3)_2$ (ml)	Amount of tartaric	Concentration of K_2CO_3
A	25.0	20	Some quantity	Un-doped
B	25.0	20	"	0.5
C	25.0	20	"	0.8
D	25.0	20	"	1.2

Drying

The samples were first treated with all glass distilled water to avoid impurities and made slurry before it was introduced into a Buckner funnel covered with filter paper then attached to a suction flask connected to the vacuum pump through its nozzle. When the pump was put on it created a vacuum that allowed for the absorption of H_2O from the sample. The filter in the Buckner funnel prevented the solid from being sucked. The sample was then taken to the oven at an appropriate temperature of 104^0C for 30 minutes. After which it was placed inside the desiccators to maintain dryness. $CaCl_2$ was used as a desiccant.

RESULTS AND DISCUSSION

(a) Optical analysis

The optical studies for the sol gel grown crystals were done using a JENWAY 6405 UV- VIS spectrophotometer operating at a wavelength range of 200nm to 1200nm at intervals of 5nm. In the optical absorption study, deionised water was used as reference. The crystal samples were dissolved in deionised water forming a colloidal solution which was then subjected to UV-VIS analysis. The graphs of the optical analyses for the grown crystals of un-doped, doped $PbCl_2$ and impurities are shown in figures 1 to 24 and the results on tables 2 and 3 below.

Figures 1-8: Optical Analysis for Un-doped and Impurity doped PbCl₂ and impurities.
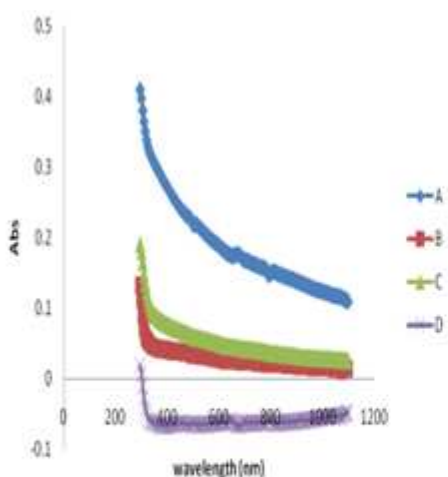
Fig. 1: Absorbance against wavelength doped (nm) $PbCl_2$
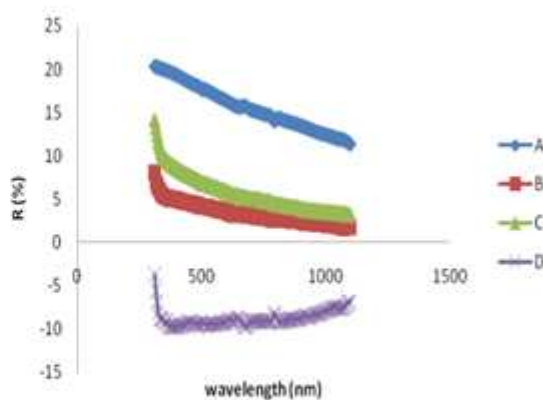
Fig. 2: Reflectance against wavelength (nm) for $PbCl_2$
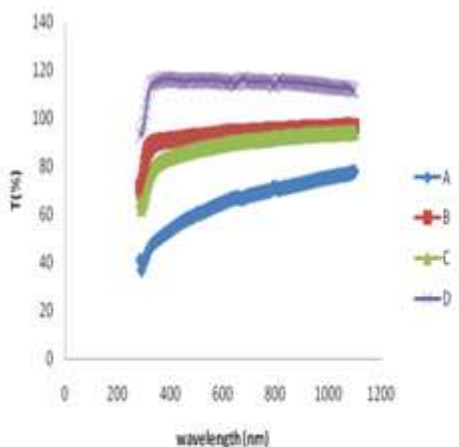
Fig. 3: Transmittance against wavelength (nm) for $PbCl_2$
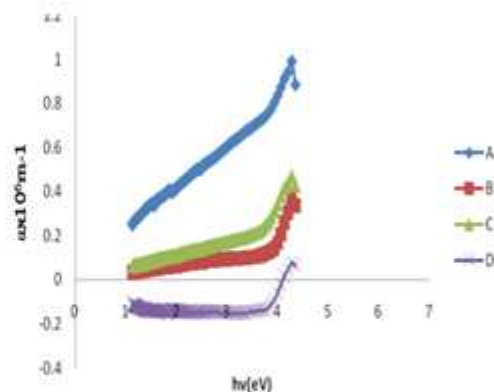
Fig. 4: Absorption Coefficient (α) vs. Photon Energy (hυ) for $PbCl_2$
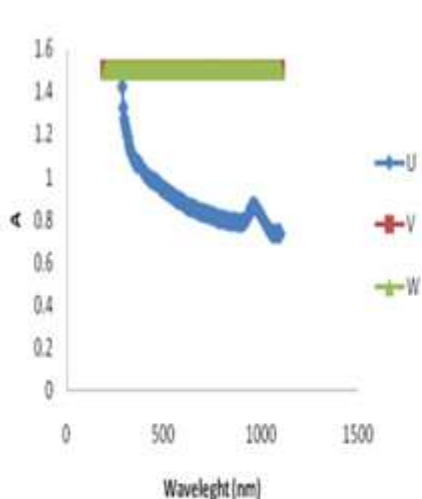
Fig. 5: A plot of absorbance (A) against wavelength (nm) for impurities.
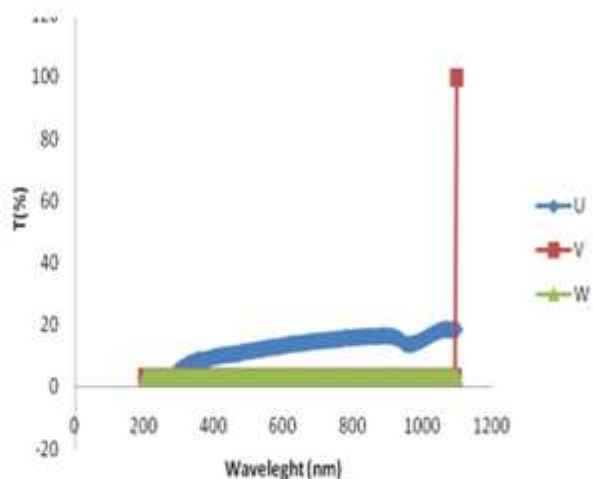
Fig. 6: A plot of transmittance (%) against wavelength (nm) for impurities.
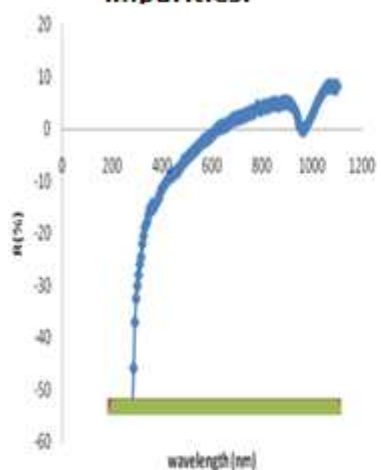
Fig. 7: A plot of reflectance (%) against wavelength (nm) for
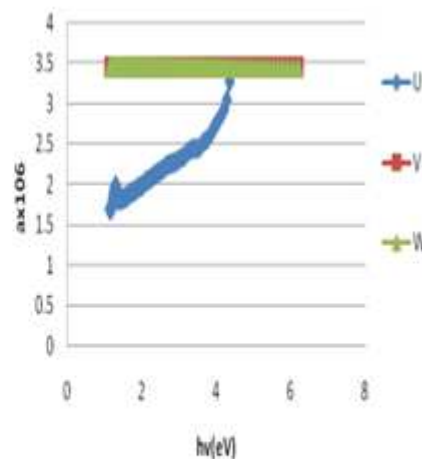
Fig. 8: A plot of absorption coefficient (α) against Photon energy (hυ) for

Table 2: Results of optical properties for un-doped and potash doped PbCl₂

S/n	Compd.	Fig.	Absorbance (A)	Transmittance (%T)	Reflectance (%R)	Absorption coefficient (a)	Usage
1	PbCl₂	1-4.	Sample A is highly absorbing in the VIS region and decreased towards the IR but B and C are moderately absorbing in the VIS and decreased towards the IR region.	Sample A is highly transmitting from the VIS to the IR regions while samples B and C are moderately transmitting in VIS region and increased towards the IR.	Samples A and B are highly reflecting in the VIS and decreased towards the IR but sample C has very low reflectance in the VIS and no reflectance nin the IR region.	Samples A and B have absorption coefficient between 0 and 1 while C has no absorption coefficient	The samples can be used in cold regions to warm rooms and in the coating of poultry roofs and walls, [11-13].
2	U- Potash, V- Bamboo, W- Raffia.		Samples V and W have very absorbance of equal strength at 1.55 from the UV to IR regions. Sample U has	Sample W has low transmittance from the VIS and increased moderately towards the NIR. Samples V and W are not transmitting from UV to NIR.	All the samples have negative reflectance. U increased towards the IR region.	Samples V and W have high absorption coefficient of equal strength of 3.5 but sample U has absorption coefficient between 1.6 to 3.5.	Sample W can be used in solar cell technology.

480

Figures 9-16: Graph of Optical constants for un-doped and doped PbCl₂ and impurities
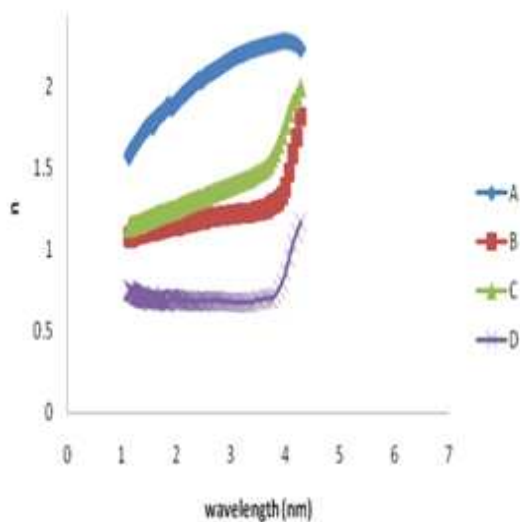
Fig. 9: Refractive Index (n) against Photon Energy (hυ) for PbCl₂
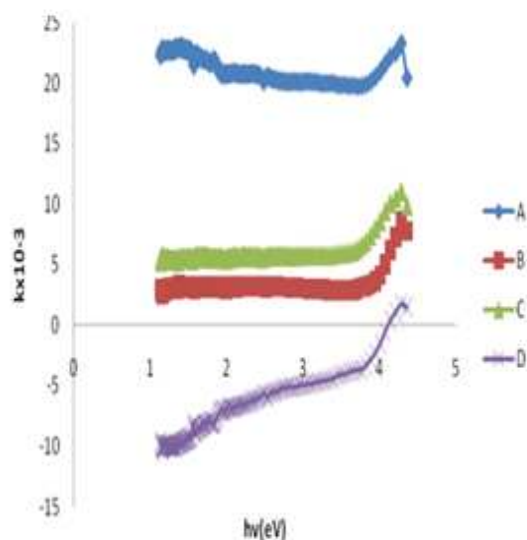
Fig. 10: Variation of extinction coefficient (k) against Photon Energy (hυ)
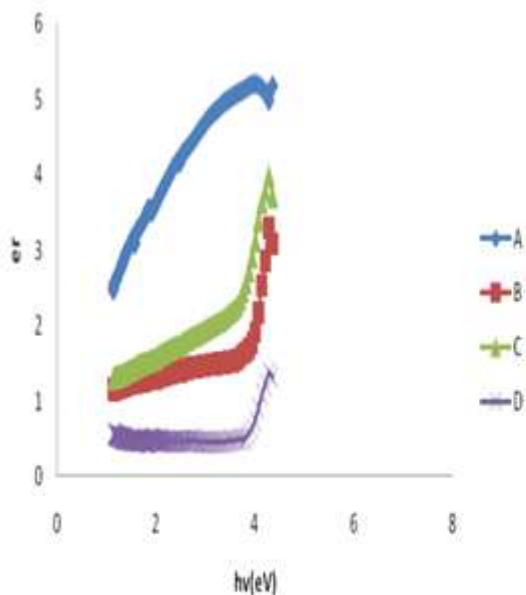
Fig. 11: Real dielectric constant (□ᵣ) with Photon energy (hυ) for PbCl₂
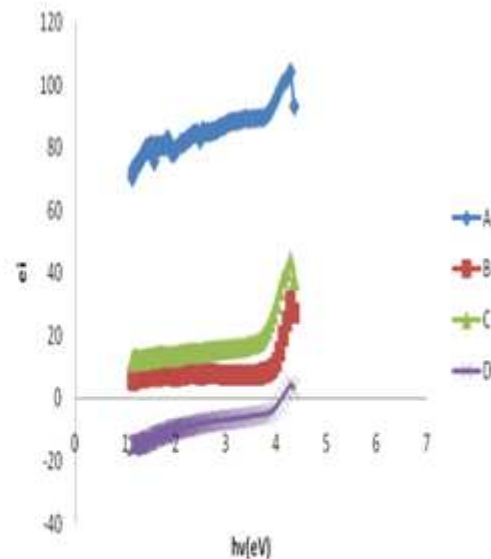
Fig. 12: Imaginary dielectric (□ᵢ) with photon energy (hυ) for PbCl₂

481
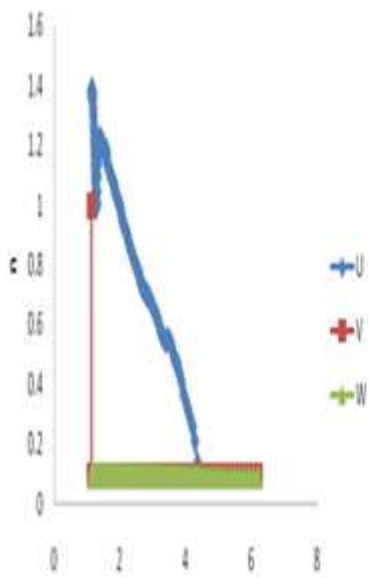
Fig. 13: A plot of refractive index against photon energy (hυ) for impurities.
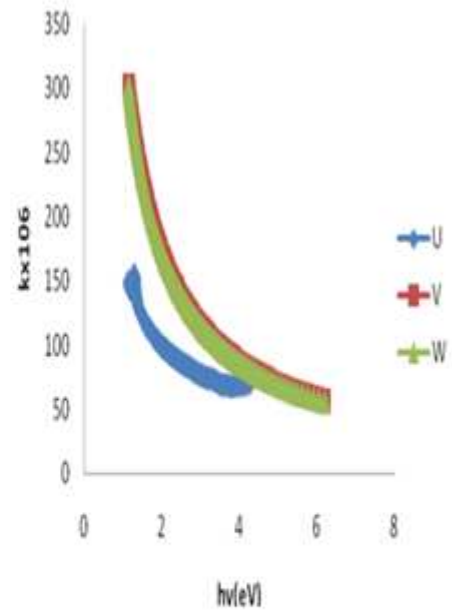
Fig. 14: A plot of extinction coefficient (k) against photon energy (hυ) for impurities.
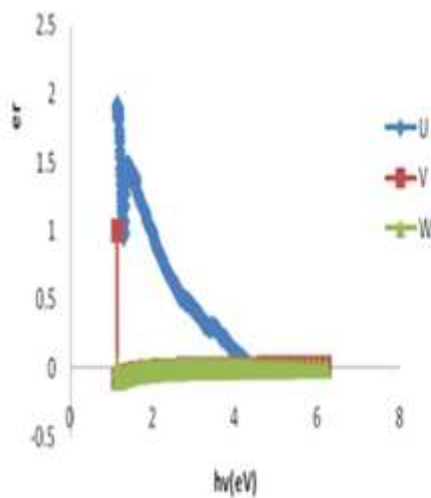
Fig. 15: A plot of real dielectric ($\square_r$) against photon energy (hυ) for impurities.
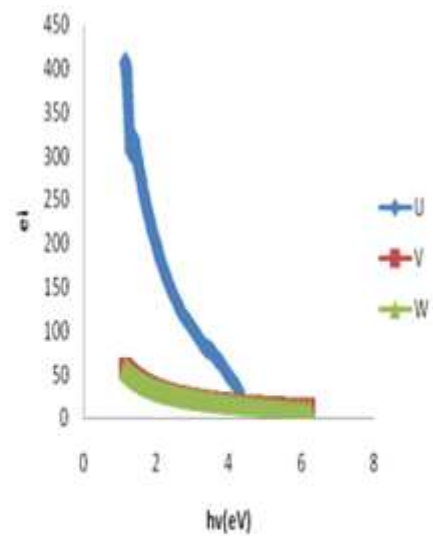
Fig. 16: A plot of imaginary dielectric ($\square_i$) against photon energy (hυ) for impurities

482

Table 3: Result for optical constant for doped and un-doped $PbCl_2$

S/n	Compound	Sample	Refractive index (n)	Extinction coefficient k	Real dielectric constant (ϵ_r)	Imaginary dielectric (ϵ_i)
1	$PbCl_2$	A B C	All the samples have very high absorption coefficient between 1 and 2.4	Sample A has the highest extinction coefficient followed by B but C has little or no extinction coefficient.	Samples A, B and C have real dielectric between 1 and 5.1.	Samples A and B have imaginary dielectric between 10 and 110 but C has C has no imaginary dielectric.
2	U-Potash, V-Bamboo, W-Raffia.		Samples U and V have equal refractive indexes between 0.1 to 1.4.	Samples V and W have equal extinction coefficient between 50 and 300 but U has absorption coefficient between 50 and 150.	Samples V and W have zero real dielectric between 0 and 2.	Samples V and W have imaginary dielectric between 0 and 50 while U lies between 0 and 425.

Figures 17-22: Optical band gaps for un-doped and doped lead chloride ($PbCl_2$)
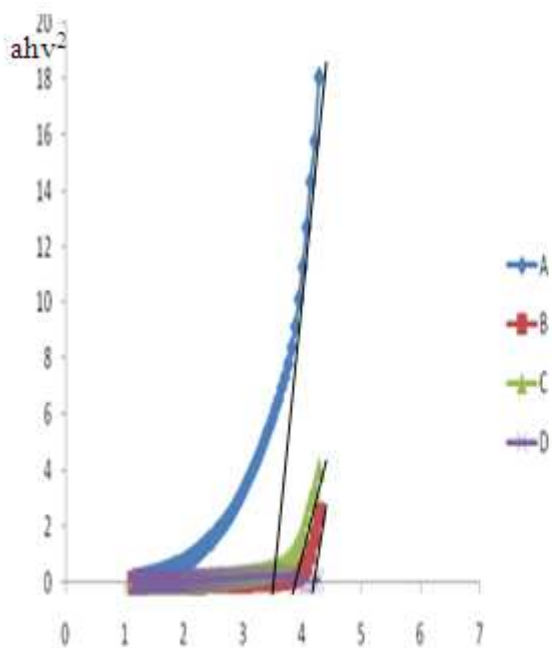
Fig. 17: A plot of $(ahv)^2$ against photon energy (hv) for $PbCl_2$.

Fig. 18: A plot of (ahʋ) against photon energy (hʋ) for $PbCl_2$.

483
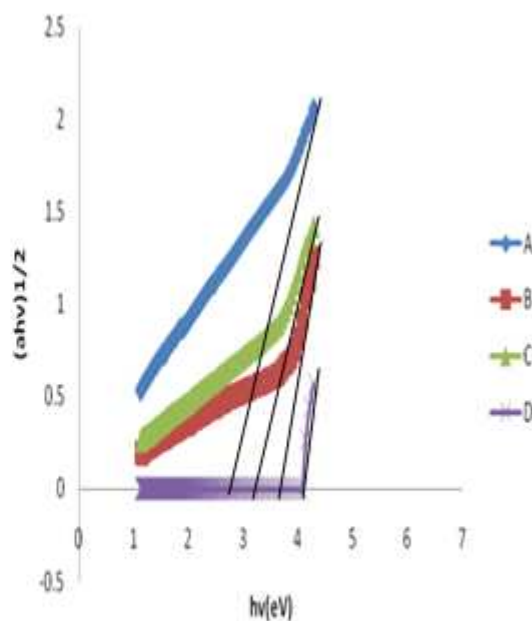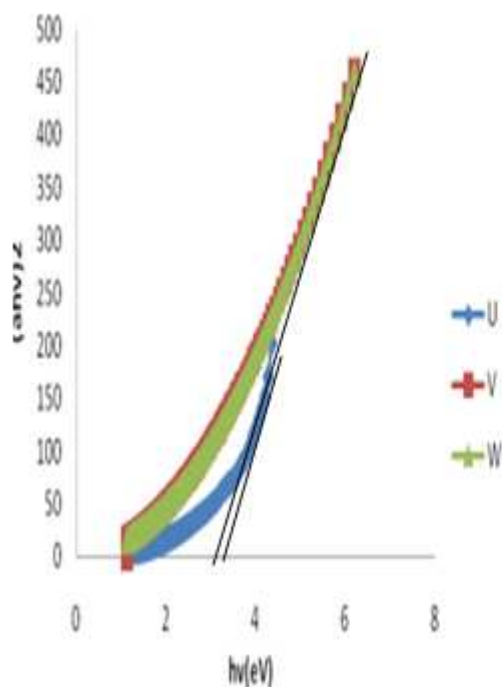
Fig. 21: A plot of (ahv)² against photon energy (hv) for impurities.
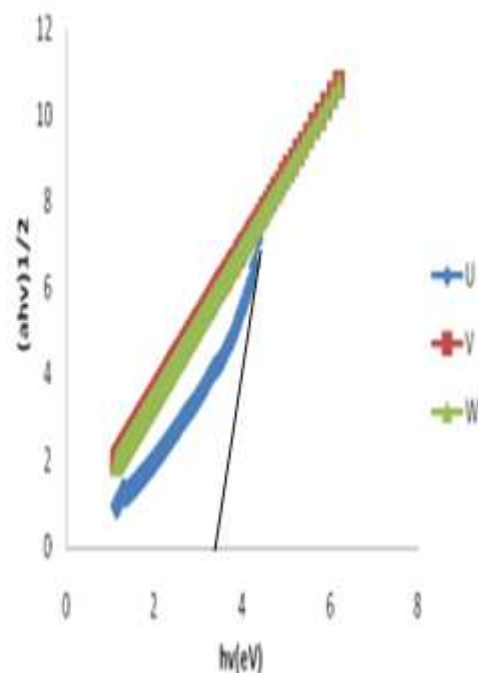
Fig. 22: A plot of (ah□)^{1/2} against photon energy (eV) for impurities.

Table 4: Result for optical band gaps for un-doped and potash doped PbCl₂

S/n	Compound	Sample	(^{L}hv)²	(^{L}hv)^½	Usage
1	PbCl₂	A	A=3.8, B=4.1, C=4.0, D=4.2.	A=2.7, B=3.75, C=3.74, D=4.0.	Wide band gap materials can be used in high power, high temperature, and high frequency and optoelectronic devices, [12,13].
	U- Potash, V-Bamboo, W- Raffia.	B	U=3.8, V=3.0, W=3.2.	U=3.4, V= 0. W=0.	Wide band gap materials can be used as refractory material and as heat sink. V and W have no indirect allowed, direct forbidden and indirect forbidden band gaps, [14].

(b) XRD Result.

X ray diffraction analysis (XRD) was used to uniquely identify the crystalline phases present in the crystals and to study the structural properties. The XRD characterization of the samples was carried out using MD-10 Diffractometer, which recorded diffractograms using CuK^L radiation. Diffraction patterns of the samples were recorded in the 2θ range from 10° to 72°. XRD spectra in figures 25–31 revealed that the compounds grown are crystalline in nature. For each spectrum, the crystallite size D, was determined using the Debye Scherer formula, [11, 12] as given below:

D=Kλ/ßcosθ ………………………………………… (1.3)

Where K = 0.9 is the shape factor, λ= 1.5409Å, θ is the diffraction peak angle (Bragg's Angle) in degrees and ß is the corresponding diffraction peak. The XRD diffractograms for un-doped, impurity doped and the local dopants are shown in figures 23 to 29. The results of the XRD analysis are shown on table 5 below.

Figures 23-29: XRD Spectra for Un-doped and Impurity PbCl₂ Crystals and the Local Dopants.
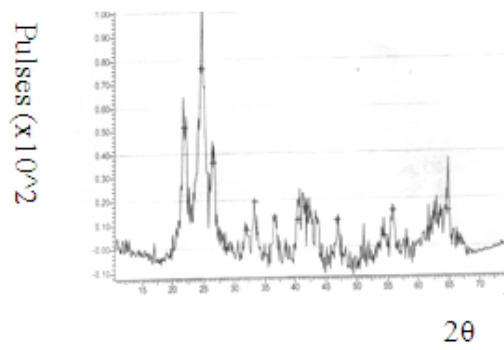
Fig. 23: XRD spectra for un-doped PbCl$_2$.
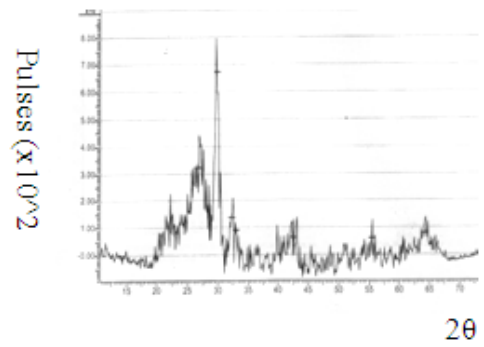
Fig. 24: XRD spectra for potash doped PbCl$_2$.
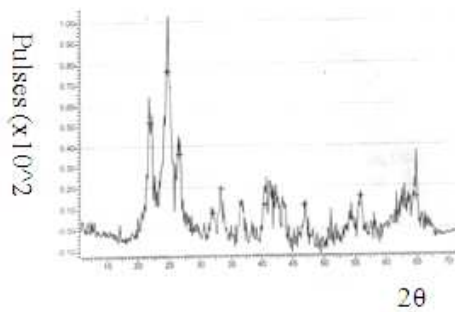
Fig. 25: XRD spectra for bamboo doped PbCl$_2$.
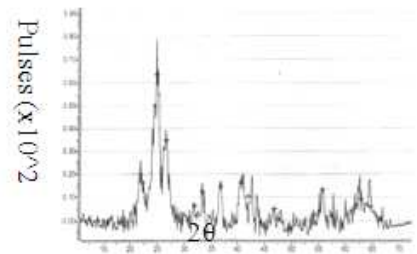
Fig. 26: XRD spectra for raffia doped PbCl$_2$.
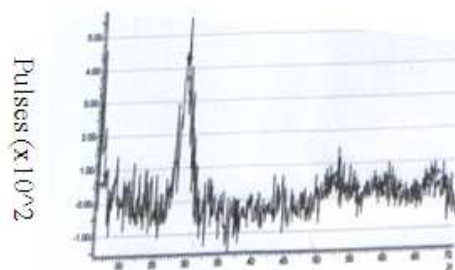
Fig. 27: XRD spectra for potash.
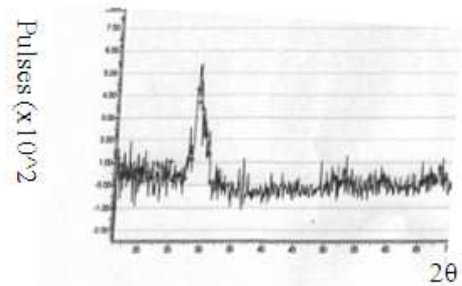
Fig. 28: XRD spectra for bamboo
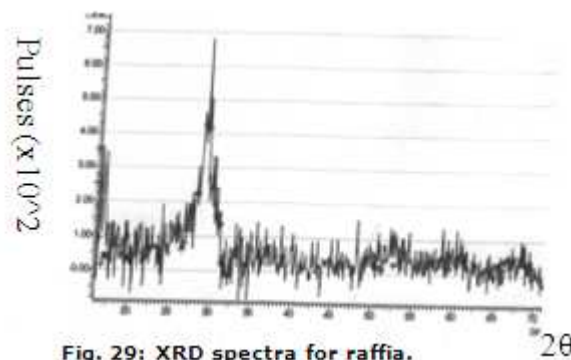
Fig. 29: XRD spectra for raffia.

Table 5: XRD results for un-doped and potash doped PbCl₂

S/n	Compound.	Sample.	Quantity.	2θ	Crystallite size (nm)	FWHM	Effect/result.
1	PbCl₂	A (un-doped)	1 pipette drop	24.59, 26.41, 28.82, 33.16.	0.7740, 1.6518, 0.2651, 1.5903.	1.7852, 0.8172, 5.2573, 0.8857.	Presence of very sharp peaks and reduced crystallite size, [15].
		B (potash) doped	1 pipette drop	29.73, 26.66, 32.20, 32.91.	1.7290, 0.3417, 1.6575, 2.3987.	0.8079, 4.0605, 0.8477, 0.5869.	Broad peak at 29.73 indicating nano crystallinity and sharp peak at 2θ at 26.66, 32.20 and 29.73 indicating crystallinity, [15].
		C (bamboo doped)	1 pipette drop	21.81, 24.64, 26.48, 31.85.	1.0847, 0.8628, 1.3595, 2.2470.	1.2675, 1.6016, 1.0201, 0.6247.	Sharp peaks indicating crystallinity and broad peaks at 21.81, 24.64 and 26.48 indicating nano crystallinitty.
		D (Raffia doped)	1 pipette	22.04, 24.72, 26.52, 31.90	0.6490, 1.0168, 1.2864, 1.6056.	2.1193, 1.3592, 1.0782, 0.8745.	Sharp and broad peaks at 22.04, 24.72 and 26.52 indicating crystallinity and nano structure.
2	Potash	Potash	1 pipette drop	17.13, 17.37, 14.25, 19.49.	2.9874, 2.9887, 2.9768, 2.9973..	0.457, 0.457, 0.457, 0.457.	2θ at 17.13 and 17.37 is potassium iron oxide; 2θ at 14.25 and 19.46 is potassium aluminum, silicate (KAlSiO₄).
3	Bamboo	Bamboo	1 pipette drop	11.26, 10.49, 13.67, 11.51.	3.2067, 3.2051, 3.2143, 3.2569.	0.423, 0.423, 0.423, 0.423.	2θ at 11.26 is Natrosilite (Na₂Si₂O₅), 2θ at 10.49 is Ungarettite (Na₃Mn₅Si₈O₂₄), 2θ at 13.67 is Clinoferrosilite (FeSiO₃) and 2 at 11.51 is Wallastonite (CaSiO₃).
4	Raffia	Raffia	1 pipette	9.88, 15.23, 18.35, 29.06.	2.7709, 2.7568, 2.7681, 2.8231.	0.494, 0.494, 0.494, 0.494.	2θ at 9.88 and 15.23 is Vanthoffite and 2θ at 18.35 and 29.06 is Iron silicate (FeSi₂)

CONCLUSION

Crystals of un-doped and impurity doped (PbCl₂) were grown using sol-gel deposition. It was discovered that

▪ The dopants in PbCl₂ affected the transparency of the material and as such offer them the opportunity to be used as a semiconductor material.
▪ The band gaps lie from 3.2 to 4.3 showing that they are refractory semi conductors and can be employed in high power, high temperature, high frequency materials, optoelectronic devices and as heat sink, [14].
▪ The reduced particle sizes from 0.8 to 3.2 are a function of broadness of the peaks and as such show that they are good nano materials, [15].
▪ The sharpness of the peaks indicates that they are highly crystalline and as such are semiconductor materials that can be employed in solar energy applications.
▪ Local materials from African environment can affect the optical and structural properties of semi conductor materials/crystals as seen in the crystallite size.
▪ XRD has shown that the aforementioned local materials are crystalline, nano polymer materials.
▪ The films have potential applications for poultry protection, solar control and antireflection coatings, [11, 12, 16].

REFERENCES

[1] Perry P, Handbook of Inorganic Compounds, **1995**, 213.
[2] Aboujali L.A, *Journal of Material Chemistry*, **1998**, 8, 1601-1606.
[3] Lowack R.H, *Journal of Organometalic Chemistry*, **1994**, 476, 25-32.
[4] Allman III R.M, UCLA School of Engineering and Applied Science, Wikipedia: the free Encyclopedia 1, **1983**.
[5] Edwards S.E, *the Nanotech Pioneers*, Wiley-VCH Verlag GMBH $ Co. KGA, Wenham, **2006**, pp. 1-5.
[6] Baries, K, the Architecture of Simon Valez, **2004**, 45.
[7] Elenga R.G, Dirias G.F, Maniongui J.G, Djemia P, Biget M.P, *Science Direct*, **2008**, 3, 31.
[8] Elena R.G, Dirias G.F, Maniongni J.G, Djemia P, Biget M.P, *Science Direct*, **2009**, 40, 418.
[9] Nichol, R.B, Potash and Phosphate Institute, **2008**, 78.
[10] Ochuenwike C.C, Unpublished M.Sc. Thesis, **1986**, 77-80.
[11] Ezema F.I, Ekwealor A.B.C, Osuji R.U, *Journal of Optoelectronics and Advanced Materials*, **2007**, 9: 1899-1902.
[12] Okpala U.V, *African Journal of Physics*, **2009**, 2:114.
[13] Okpala U.V, Ezema F.I, Osuji R.U, *Advances in Applied Science Research*, **2012**, 3(1):105.
[14] Yacobi B.G, *Semiconductor Materials*, Kluwer Academic Publisher, New York, **2004**, pp.148-151.

[15] Kondawar S.B, *Arch.Appl. Sci.Res*, **2010**, 2(3) 225-230.
[16] Ezema F.I, *Journal of Applied Sciences*, **2006**, 6(8) 1827-1823.